Materials Science Forum Vols. 638-642 (2010) pp 1878-1883
Online available since 2010/Jan/12 at www.scientific.net

doi:10.4028/www.scientific.net/MSF.638-642.1878

A Theoretical and Experimental Study on the Dynamic Constitutive Model of Aluminum Foams

YU Jilin[1, a], WANG Erheng[1,b] and GUO Liuwei[1,c]

[1]CAS Key Laboratory of Mechanical Behavior and Design of Materials, University of Science and Technology of China, Hefei, Anhui 230027, People's Republic of China

[a]jlyu@ustc.edu.cn, [b]erhengwang@gmail.com, [c]glwhn@mail.ustc.edu.cn

Keywords: Aluminum foams, Compression tests, Dynamic Constitutive Model, Lateral constraint.

Abstract. The phenomenological constitutive framework for compressible elasto-plastic solids presented by Chen and Lu [1] is extended to the dynamic cases by assuming that the material parameter curves in the stress potential depend also on the strain rate. To check the applicability of the extended model, three types of dynamic experiments, i.e., uniaxial compression, lateral-constrained compression and side-constrained compression tests, are conducted for an open-cell aluminum foam at different strain rates. The first two types of dynamic tests are used as characteristic tests to determine the material parameter curves at different strain rates which are then used to construct the stress potential function in the model. The results show that the stress-strain curves under side-constrained compression predicted by the model are in agreement with those obtained experimentally.

Introduction

Low density metal foams are new materials with promising mechanical, thermal and acoustical properties. A wide range of engineering applications is under exploration. In the numerical simulation and design of engineering structures using metal foam and foam-based components, constitutive models for the foam are required.

Considering the compressibility, the geometry imperfections, the complexity of microstructures, and the variety of failure behaviors [2-5], a macro-mechanical model of metal foams is extremely demanded in engineering applications. A yield surface was derived from the analysis of an idealistic metal foam element by Gibson et al [6]. A self-similar yield surface model and a differential hardening model were proposed by Deshpande and Fleck [7], based on the quadratic yielding surface in the mean stress versus effective stress space found in their experiments. By incorporating the yield surface of metal foams derived in [6], Miller [8] extended the Drucker-Prager model and proposed an isotropic constitutive model. There were also other constitutive models in the literature and finite element codes. These models have different formulations for the yield surface, hardening rule and plastic flow rule. A survey of nine constitutive models claiming to be applicable for structural considerations of aluminum foams was given by Hanssen et al [9] where experimental and numerical validations of some constitutive models were performed.

A framework of constructing phenomenological constitutive models for elasto-plastic materials was presented by Chen and Lu [1]. A stress potential based on characteristic stress and total strain was proposed, which differs from the conventional yield function as no attempt is made to separate elastic strains from plastic deformations. The stress potential and the associated constitutive model were characterized by a set of multiaxial tests. No information about the initial yield surface and its evolution was required. It was shown in our previous quasi-static experimental investigation on an open-call aluminum foam and a closed-cell aluminum foam [10] that this model could describe the compression-dominant behavior of the foams well.

The dynamic response of metal foams is also very important for some engineering applications, especially those related to impact and energy absorption. Unfortunately, while many research works have been reported for the uniaxial compression behavior of aluminum foams under different strain rates, no dynamic constitutive model is available in the literature. In this paper, we extend the phenomenological constitutive framework presented by Chen and Lu in Ref. [1] to the dynamic cases for metal foams and apply the dynamic constitutive model to an open-cell aluminum foam. Three types of dynamic tests were performed and the experimental results are used to validate the model.

Theoretical Model

Characteristic Stress and Characteristic Strain. The assumption made in Ref. [1] is that the material is isotropic and rate-independent. The characteristic stress and characteristic strain are introduced as follows:

$$\bar{\sigma}^2 = \sigma_e^2 + \beta^2 \sigma_m^2, \quad \bar{\varepsilon}^2 = \varepsilon_e^{\,2} + \frac{\varepsilon_v^{\,2}}{\beta^2}, \tag{1}$$

where σ_e and σ_m are the Mises effective stress and mean stress, ε_e and ε_v are the Mises effective strain and mean strain, respectively. It can be verified that $\bar{\sigma}$ is related to $\bar{\varepsilon}$ by

$$\bar{\sigma} = \bar{E}\bar{\varepsilon}, \tag{2}$$

where $\bar{E}$ and β are material parameters defined as

$$\bar{E} = \frac{3E}{2(1+\nu)}, \quad \beta^2 = \frac{9(1-2\nu)}{2(1+\nu)}, \tag{3}$$

where E and ν are Young's modulus and Poisson's ratio, respectively.

Under uniaxial compression, $\bar{\sigma}_{uc}$ and $\bar{\varepsilon}$ are simplified as

$$\bar{\sigma}_{uc} = \frac{1}{3}\sqrt{9+\beta^2}\,|\sigma_u|, \quad \bar{\varepsilon} = \frac{3|\varepsilon_u|}{\sqrt{9+\beta^2}}, \tag{4}$$

where σ_u and ε_u are, respectively, the axial stress and strain under uniaxial compression.

Lateral-Constrained Condition. The stress and strain under this condition are

$$\begin{aligned} &\varepsilon_{11} = \varepsilon, \ \ \varepsilon_{22} = \varepsilon_{33} = 0, \ \ \varepsilon_{12} = \varepsilon_{23} = \varepsilon_{13} = 0, \\ &\sigma_{11} = k\sigma, \ \ \sigma_{22} = \sigma_{33} = \sigma, \ \ \sigma_{12} = \sigma_{23} = \sigma_{13} = 0, \ \ (k \ge 0). \end{aligned} \tag{5}$$

This is a non-proportional loading condition that $k = k(\bar{\varepsilon})$. $\bar{\sigma}$ and $\bar{\varepsilon}$ under this condition can be obtained as

$$\bar{\sigma}_{lc}^2 = [(k-1)^2 + \frac{\beta^2}{9}(k+2)^2]\sigma^2, \quad \bar{\varepsilon}^2 = (\frac{4}{9} + \frac{1}{\beta^2})\varepsilon^2. \tag{6}$$

Stress Potential Function. The following stress potential function Φ is proposed by Chen and Lu for cellular metal foams:

$$\Phi = \bar{\sigma}^2 + C(\bar{\varepsilon})\sigma_{\mathrm{m}}^2 - \mathrm{Y}(\bar{\varepsilon}) = 0, \tag{7}$$

where $C(\bar{\varepsilon})$ and $Y(\bar{\varepsilon})$ are two material parameters to be determined by characteristic experiments. We extend this model to dynamic cases by introducing the strain-rate effect into Eq. 7 that

$$\Phi = \bar{\sigma}^2 + C(\bar{\varepsilon},\dot{\varepsilon})\sigma_{\mathrm{m}}^2 - \mathrm{Y}(\bar{\varepsilon},\dot{\varepsilon}) = 0, \tag{8}$$

where $C(\bar{\varepsilon},\dot{\varepsilon})$ and $Y(\bar{\varepsilon},\dot{\varepsilon})$ are to be determined by two sets of dynamic tests, e.g. uniaxial and lateral-constrained compression tests. In this case we have

$$\begin{aligned} C(\bar{\varepsilon},\dot{\varepsilon}) &= \frac{(9+\beta^2)\{9k^2\bar{\sigma}_{uc}^2(\bar{\varepsilon},\dot{\varepsilon}) - [9(k-1)^2+\beta^2(k+2)^2]\bar{\sigma}_{lc}^2(\bar{\varepsilon},\dot{\varepsilon})\}}{(9+\beta^2)(k+2)^2\bar{\sigma}_{lc}^2(\bar{\varepsilon},\dot{\varepsilon}) - 9k^2\bar{\sigma}_{uc}^2(\bar{\varepsilon},\dot{\varepsilon})}, \\ \mathrm{Y}(\bar{\varepsilon},\dot{\varepsilon}) &= \frac{27(2k+1)\bar{\sigma}_{uc}^2(\bar{\varepsilon},\dot{\varepsilon})\bar{\sigma}_{lc}^2(\bar{\varepsilon},\dot{\varepsilon})}{(9+\beta^2)(k+2)^2\bar{\sigma}_{lc}^2(\bar{\varepsilon},\dot{\varepsilon}) - 9k^2\bar{\sigma}_{uc}^2(\bar{\varepsilon},\dot{\varepsilon})}, \end{aligned} \tag{9}$$

where subscripts uc and lc denote the uniaxial and lateral-constrained compression tests respectively, and $k \equiv \sigma_{11}/\sigma_{22} = k(\bar{\varepsilon},\dot{\varepsilon})$, which is associated with the lateral-constrained condition and need to be solved simultaneously.

Under the lateral-constrained condition, we have $d\varepsilon_{22} = d\varepsilon_{33} = 0$, and it can be approved that

$$k = k(\bar{\varepsilon},\dot{\varepsilon}) = -\frac{9+4\beta^2+4C(\bar{\varepsilon},\dot{\varepsilon})}{-9+2\beta^2+2C(\bar{\varepsilon},\dot{\varepsilon})}, \tag{10}$$

which, using Eq. 9, leads to

$$k = -\frac{1}{2} + \frac{1}{2}\sqrt{1+\frac{8(9+\beta^2)}{9-9S+\beta^2}}, \tag{11}$$

where $S = \bar{\sigma}_{uc}^2/\bar{\sigma}_{lc}^2$.

Thus, $C(\bar{\varepsilon},\dot{\varepsilon})$ and $Y(\bar{\varepsilon},\dot{\varepsilon})$ can be obtained from Eqs. 9 and 11 when the stress-strain curves in uniaxial and lateral-constrained compression tests under different strain-rates are available. It is assumed that the stress potential function, Eq. 8, can be used in conjunction with the associated flow rule to give the total strain rate as

$$\dot{\varepsilon}_{ij} = \dot{\lambda}\frac{\partial\Phi}{\partial\sigma_{ij}}, \tag{12}$$

where the proportionality factor $\dot{\lambda}$ is determined from the consistence condition of plasticity as

$$\dot{\Phi} = \frac{\partial\Phi}{\partial\sigma_{ij}}\dot{\sigma}_{ij} + \frac{\partial\Phi}{\partial\bar{\varepsilon}}\dot{\bar{\varepsilon}} = \frac{\partial\Phi}{\partial\sigma_{ij}}\dot{\sigma}_{ij} + \frac{\partial\Phi}{\partial\bar{\varepsilon}}\frac{\partial\bar{\varepsilon}}{\partial\varepsilon_{ij}}\dot{\varepsilon}_{ij} = 0. \tag{13}$$

Side-Constrained Condition. The stress and strain tensors under the side-constrained condition are as follows:

$$\begin{aligned}&\sigma_{11}=\sigma_1,\ \ \sigma_{22}=0,\ \ \sigma_{33}=\sigma_3,\ \ \sigma_{12}=\sigma_{23}=\sigma_{13}=0,\\&\varepsilon_{11}=\varepsilon_1,\ \ \varepsilon_{22}=\varepsilon_2,\ \ \varepsilon_{33}=0,\ \ \varepsilon_{12}=\varepsilon_{23}=\varepsilon_{13}=0.\end{aligned} \tag{14}$$

From Eqs. 12 and 13, in conjunction with Eqs. 1 and 14, we get

$$\begin{aligned}d\varepsilon_{11}&=-\frac{\partial\Phi}{\partial\sigma_{11}}\frac{\dfrac{\partial\Phi}{\partial\sigma_{11}}d\sigma_{11}+\dfrac{\partial\Phi}{\partial\sigma_{33}}d\sigma_{33}}{\dfrac{\partial\Phi}{\partial\bar{\varepsilon}}(\dfrac{\partial\Phi}{\partial\sigma_{km}}g_{km})},\\d\varepsilon_{22}&=-\frac{\partial\Phi}{\partial\sigma_{22}}\frac{\dfrac{\partial\Phi}{\partial\sigma_{11}}d\sigma_{11}+\dfrac{\partial\Phi}{\partial\sigma_{33}}d\sigma_{33}}{\dfrac{\partial\Phi}{\partial\bar{\varepsilon}}(\dfrac{\partial\Phi}{\partial\sigma_{km}}g_{km})},\\d\varepsilon_{33}&=-\frac{\partial\Phi}{\partial\sigma_{33}}\frac{\dfrac{\partial\Phi}{\partial\sigma_{11}}d\sigma_{11}+\dfrac{\partial\Phi}{\partial\sigma_{33}}d\sigma_{33}}{\dfrac{\partial\Phi}{\partial\bar{\varepsilon}}(\dfrac{\partial\Phi}{\partial\sigma_{km}}g_{km})},\end{aligned} \tag{15}$$

where

$$\begin{aligned}&\frac{\partial\bar{\varepsilon}}{\partial\varepsilon_{11}}=\frac{1}{\bar{\varepsilon}}[(\frac{4}{9}+\frac{1}{\beta^2})\varepsilon_1+(\frac{1}{\beta^2}-\frac{2}{9})\varepsilon_2]=g_{11},\ \ \frac{\partial\bar{\varepsilon}}{\partial\varepsilon_{22}}=\frac{1}{\bar{\varepsilon}}[(\frac{4}{9}+\frac{1}{\beta^2})\varepsilon_2+(\frac{1}{\beta^2}-\frac{2}{9})\varepsilon_1]=g_{22},\\&\frac{\partial\bar{\varepsilon}}{\partial\varepsilon_{33}}=\frac{1}{\bar{\varepsilon}}(\frac{1}{\beta^2}-\frac{2}{9})(\varepsilon_1+\varepsilon_2)=g_{33},\ \ \frac{\partial\Phi}{\partial\sigma_{11}}=(2\sigma_1-\sigma_3)+\frac{2(\beta^2+C)}{9}(\sigma_1+\sigma_3),\\&\frac{\partial\Phi}{\partial\sigma_{22}}=[\frac{2(\beta^2+C)}{9}-1](\sigma_1+\sigma_3),\ \ \frac{\partial\Phi}{\partial\sigma_{33}}=(2\sigma_3-\sigma_1)+\frac{2(\beta^2+C)}{9}(\sigma_1+\sigma_3).\end{aligned} \tag{16}$$

Since $d\varepsilon_{33}=0$ and consequently $\partial\Phi/\partial\sigma_{33}=0$, the relationship between σ_1 and σ_3 can be obtained from Eq. 16. On the other hand, from Eq. 15 we have $\dfrac{d\varepsilon_{11}}{d\varepsilon_{22}}=\dfrac{\partial\Phi}{\partial\sigma_{11}}\Big/\dfrac{\partial\Phi}{\partial\sigma_{22}}$, the relationship between ε_{11} and ε_{22} can also be obtained. So the relationship between $\bar{\sigma}$ and σ_1, and that between $\bar{\varepsilon}$ and ε_1 are established. Finally, the stress and strain curve under side-constrained compression condition can be predicted by the model using the stress potential function.

Experimental Results and Discussion

The above dynamic constitutive model is validated by experiments using an open-cell aluminum foam. Three types of dynamic experiments, i.e., uniaxial compression, lateral-constrained compression and side-constrained compression tests, are conducted under quasi-static condition and

dynamic conditions at three different strain rates. The experimental setup and parameters used in the experiments are detailed in Ref. [11]. Here we only show some typical results.

The stress-strain curves obtained experimentally under different constraint conditions are shown in Fig.1. The material parameter curves $C(\bar{\varepsilon},\dot{\varepsilon})$ and $Y(\bar{\varepsilon},\dot{\varepsilon})$ at different strain rates determined from the uniaxial and lateral-constrained compression tests are shown in Fig.2. It is obvious that $C(\bar{\varepsilon},\dot{\varepsilon})$ under dynamic condition is different from that under quasi-static condition.

To validate the dynamic constitutive model presented in the previous section, these material parameter curves are used in the model to predict the stress-strain response of the open-cell aluminum foam under side-constrained condition. A comparison of the result with that obtained experimentally at a strain rate of 1400/s is shown in Fig.3. Although the curve predicted by the model is slightly lower than that of experiments, the trend of two curves is consistent. In considering the fact that metal foams are highly heterogeneous with large dispersion in strength, the agreement is good.

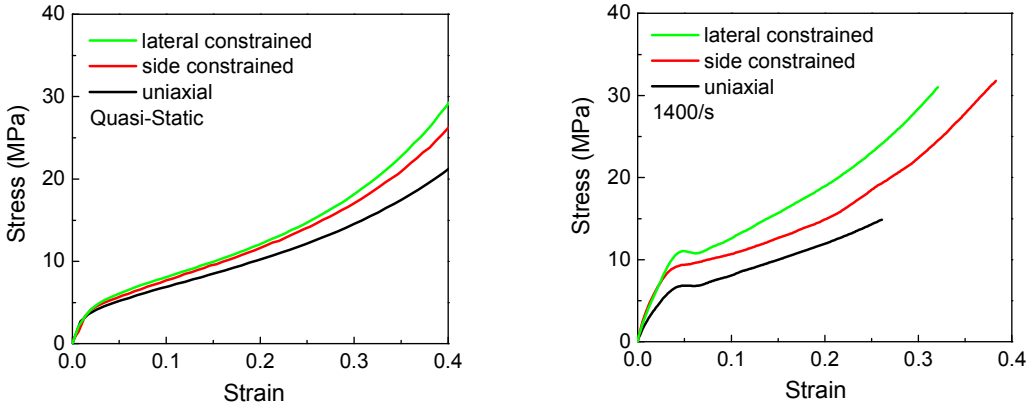

Fig.1. Axial stress-strain curves of the open-cell aluminum foam under (a) quasi-static and (b) dynamic loading

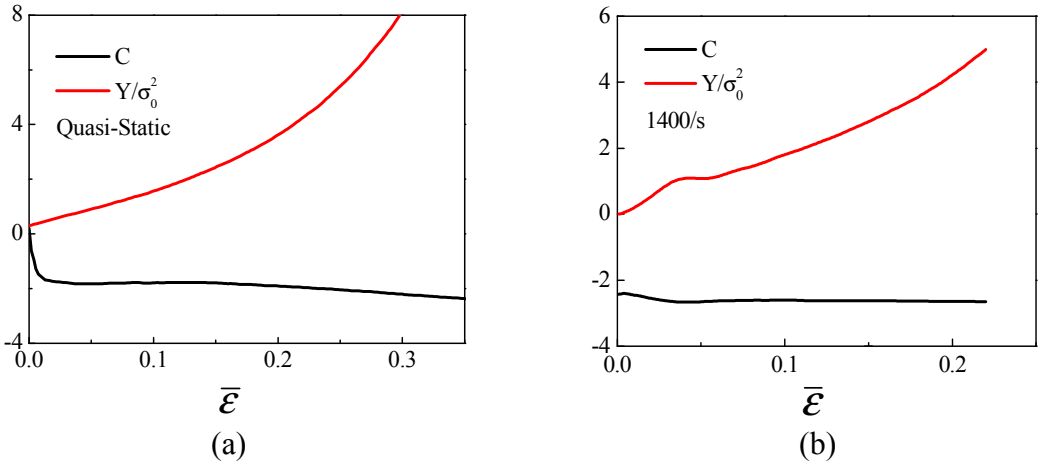

Fig.2. The material parameter cuves $C(\bar{\varepsilon},\dot{\varepsilon})$ and $Y(\bar{\varepsilon},\dot{\varepsilon})$ at different strain rates

Conclusion

In this paper, the model proposed by Chen and Lu for compressible solids is extended to the dynamic cases for metal foams by assuming that the material parameter curves in the stress potential depend also on the strain rate. The expressions of the dynamic constitutive model are presented. Three types

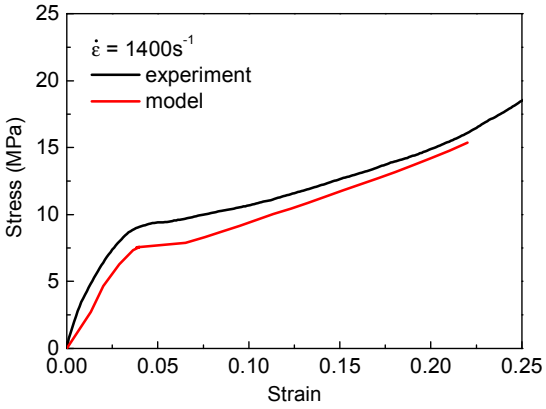

Fig.3. Comparison of the axial stress-strain curves of the open-cell aluminum foam under side-constrained dynamic compression

of dynamic compression tests, i.e., uniaxial compression, lateral-constrained compression and side-constrained compression, are conducted for an open-cell aluminum foam. The first two of them are used to obtain the material parameter curves required in the constitutive model. The results are then used to predict the dynamic response of the foam under side-constrained compression. It is found that the axial stress-strain curve of the foam under side-constrained compression predicted by the extended model is in good agreement with the experimental results. So, we conclude that the present constitutive model could be used to predict the compression-dominated dynamic behavior of the aluminum foam under investigation well.

References

[1] C. Chen and T.J. Lu: Int. J. Solids Struct. Vol. 37 (2000), p. 7769

[2] L.J. Gibson and M.F. Ashby: *Cellular Solids: Structure and Properties* (2nd ed., Cambridge University Press, Cambridge 1997).

[3] M.F. Ashby, A.G. Evans, N.A. Fleck, L.J. Gibson, J.W. Hutchinson and H.N.G. Wadley: *Metal Foams: A Design Guide* (Butterworth-Heinemann, Boston 2000).

[4] G. Gioux, T.M. McCormack and L.J. Gibson: Int. J. Mech. Sci. Vol. 42 (2000), p.1097

[5] C. Chen, T.J. Lu and N.A. Fleck: J. Mech. Phys. Solids Vol. 47 (1999), p. 2235

[6] L.J. Gibson, F.M. Ashby, J. Zhang and T.C. Triantafillou: Int. J. Mech. Sci. Vol. 31 (1989), p. 635

[7] V.S. Deshpande and N.A. Fleck: J. Mech. Phys. Solids Vol. 48 (2000), p. 1253

[8] R.E. Miller: Int. J. Mech. Sci. Vol. 42 (2000), p. 729

[9] A.G. Hanssen, O.S. Hopperstad, M. Langseth and H. Ilstad: Int. J. Mech. Sci. Vol. 44 (2002), p. 359

[10] E.H. Wang, J.L. Yu, F. Wang and L. Sun: Acta Mechanica Sinica Vol. 36 (2004), p. 673 (in Chinese)

[11] E.H. Wang, Ph.D Dissertation, University of Science and Technology of China. (2005) (in Chinese)

THERMEC 2009
10.4028/www.scientific.net/MSF.638-642

A Theoretical and Experimental Study on the Dynamic Constitutive Model of Aluminum Foams

10.4028/www.scientific.net/MSF.638-642.1878

DOI References

[1] C. Chen and T.J. Lu: Int. J. Solids Struct. Vol. 37 (2000), p. 7769
doi:10.1016/S0020-7683(00)00003-2

[4] G. Gioux, T.M. McCormack and L.J. Gibson: Int. J. Mech. Sci. Vol. 42 (2000), p.1097
doi:10.1016/S0020-7403(99)00043-0

[5] C. Chen, T.J. Lu and N.A. Fleck: J. Mech. Phys. Solids Vol. 47 (1999), p. 2235
doi:10.1016/S0022-5096(99)00030-7

[7] V.S. Deshpande and N.A. Fleck: J. Mech. Phys. Solids Vol. 48 (2000), p. 1253
doi:10.1016/S0022-5096(99)00082-4

[8] R.E. Miller: Int. J. Mech. Sci. Vol. 42 (2000), p. 729
doi:10.1016/S0020-7403(99)00021-1